N72-26466
NASA TM X- 68073

NASA TECHNICAL MEMORANDUM

NASA TM X- 68073

CHANGE IN TRANSMITTANCE OF FUSED SILICA AS A MEANS OF DETECTING MATERIAL SPUTTERED FROM COMPONENTS ON A 5-CM ION THRUSTER

by A. J. Weigand and M. J. Mirtich
Lewis Research Center
Cleveland, Ohio
May, 1972

This information is being published in preliminary form in order to expedite its early release.

CHANGE IN TRANSMITTANCE OF FUSED SILICA AS A MEANS OF DETECTING MATERIAL SPUTTERED FROM COMPONENTS ON A 5-CM ION THRUSTER

by A. J. Weigand and M. J. Mirtich

Lewis Research Center

E-6964

SUMMARY

Two endurance tests of a 5-cm mercury bombardment thruster are reported. Both tests used a translational screen-grid system with the beam vectored 10 degrees. The first test lasted 141 hours and the second test operated for 2026 hours.

In each test two fused silica samples (solar cell covers) 2.0 cm by 2.1 cm were placed in shielded holders to detect materials sputtered from the thruster. Spectral optical properties between 0.398 and 2.16 μm were measured on each sample, both before and after the endurance tests. The deposition on each sample was spectrographically analyzed to determine the type of materials sputtered from the thruster.

It was found that sputtering from the neutralizer is highly dependent on its position with respect to the beam edge. The sputtering from the accelerator grid of the translational screen-grid system of the 2026 hour test was sufficient to form an opaque film on the sample located in the direction opposite to the vectored beam.

INTRODUCTION

Ion thrusters will be used in the near future not only to send spacecraft to distant planets, but also to provide stationkeeping and attitude control of Earth orbiting satellites. For such missions the ion thrusters must be operational for long periods of time. Because of the thrusting

times involved, sputtered thruster component material may deposit on other parts of the spacecraft. These deposits could change the output of solar cells, change the transmittance of optical windows on board the spacecraft, and even change the optical properties of the thermal control coating of the spacecraft itself. In order for spacecraft designers to shield for these possibilities, it is necessary to determine (1) the source of the sputtered material, (2) the flux of the material deposited, and (3) its effect on the spacecraft surfaces of interest.

To answer experimentally some of the above problems, fused silica (solar cell cover plates) were used to collect materials sputtered from 5-cm diameter thruster components. By putting the samples in various locations near the thruster, the source of sputtering could be determined. Two plates were used in each of the endurance tests reported. Both endurance tests used a translational screen-grid system as means of extracting the ion beam. The spectral transmittance of each sample was measured both before and after the tests. Spectral data were taken between 0.398 and 2.16 μm. The samples were spectrographically analyzed to determine the elements present in the deposition. The results of the experimental investigation are reported herein.

APPARATUS AND PROCEDURE

The basic design of the 5-cm diameter thruster is shown in figure 1. For the two endurance tests, all thruster components were the same including the elements that extract the ions from the discharge chamber. The extraction system was a translational screen-grid vectoring system. The accelerator and screen grids are match-drilled molybdenum sheets as shown in figure 2. A more detailed account of the design of the translational screen-grid system is found in reference 1. The grids were assembled to provide 10-degree vectoring during both tests.

The vertically oriented vacuum tank in which all testing was performed was cylindrical in shape, 1.4 meters in diameter and 2.3 me-

ters high (fig. 3). The thruster was mounted on the top port. A frozen mercury target was located at the bottom of the tank to prevent condensible metal backsputter from the tank. In addition glass fiber baffles were located on the sides of the wall and positioned 45 degrees from the horizontal position. These implementations helped to assure that the deposition effects investigated herein originated from thruster components. A tank pressure of 1×10^{-6} psi was maintained throughout both tests.

To more fully understand the sputtering patterns of the 5-cm diameter ion thruster, two fused silica plates (typical solar cell cover slides) were placed near the thruster to collect sputtered material. The plates were 2 cm by 2.1 cm and 0.15 cm thick. They had an antireflective coating on the side that was exposed to the sputter deposition and an ultraviolet coating which filtered all radiation below 350 μm on the other side. To assure that the samples were free of contaminants the samples were cleaned with freon using an ultrasonic cleaner before being put in the tank.

To further limit the effects of material sputtered from the tank the sample plates were put in stainless steel containers that were 3.12 cm (1.25 in.) by 2.54 cm (1 in.) by 2.54 cm (1 in.). The holders had a slit 1.25 cm (0.5 in.) by 0.47 cm (0.187 in.) to allow thruster component sputtered material to enter. The samples were held in place on the back of the holder by means of metal tabs.

For the 141 hour test (test 1), the fused silica samples were located on opposite sides of the thruster diameter. The slits were in the plane of the ground screen mask which is downstream of the accelerator grid (fig. 4). This allowed a view factor for the samples to see material sputtered from thruster components only. The neutralizer was located approximately half way between the samples. As shown in figure 4, sample A is on the left in the direction of beam vectoring and sample B on the right of the neutralizer when looking toward the accelerator from a downstream position. Figure 5 is a photograph showing the samples and their locations relative to the thruster. The neu-

tralizer was 5.1 cm downstream of the accelerator grid and 2.5 cm radially away from the last row of accelerator holes. The neutralizer axis made a 15° angle with the thruster axis.

Figure 6 is a sketch of the location of the fused silica samples for the 2026 hour test (test 2). Figures 7 and 8 are photographs of the samples and their location relative to the thruster for two different views. The sample plates, as in test 1, were also in the plane of the ground screen mask. Sample A was positioned in the direction of beam vectoring. Sample B was located next to the neutralizer and the view factor to the neutralizer was zero. This position was warranted (as will be pointed out later) by the results of the first test. The neutralizer was 5.1 cm downstream of the grid and was moved to a new position 4.3 cm radially out for this test. The neutralizer axis was parallel to the thruster axis.

At the end of each endurance test, the orientation of the samples and sputter deposition patterns on them were documented. The optical properties of the samples were determined next. By using a system that included a monochromator and integrating sphere, the spectral transmittance τ was measured between 0.398 μm and 2.16 μm. (Transmittance below 0.398 μm approaches zero since the ultraviolet coating on the samples starts to cut off transmitted radiation below 0.398 μm.) The data were taken at wavelengths which corresponded to 2 percent energy increments of the Johnson curve of spectral irradiance versus wavelength. Reference 2 gives the details of this program. A simple averaging of the spectral transmittance data yields the total transmittance.

A more detailed analysis was performed on the samples from test 2. The same optical system was used to measure the sum of the transmittance and reflectance $(\tau + \rho)$. With this measurement, along with transmittance data, it is possible to calculate ρ and the absorptance α both spectrally and totally.

To determine the effect of the change in spectral transmittance of cover plates on the response of solar cells, the characteristic spectral

response of a typical 10 ohm-cm N/P silicon solar cell was used. The spectral response of this solar cell is given in figure 9 (ref. 3). From the figure it can be seen that the region of active response of a typical 10 ohm-cm N/P silicon cell is between 0.45 and 1.10 μm. By knowing the spectral transmittance of the cover plates (fused silica) at each wavelength and the spectral response of a N/P silicon solar cell, the normalized solar cell response can be determined both before and after sputter deposition by using the following equation:

$$J = \frac{\int_{\lambda_1}^{\lambda_2} J(\lambda)T(\lambda)d\lambda}{\int_{\lambda_1}^{\lambda_2} J(\lambda)d\lambda} \qquad (1)$$

where λ_1 and λ_2 are the initial and final wavelengths of the response curve respectively (0.45 and 1.10 for these data). $J(\lambda)$ is the spectral response of the solar cell at each wavelength, and $T(\lambda)$ is the spectral transmittance of the fused silica.

The final examination of the samples consisted of spectrographically analyzing each sample. This technique allows one to determine the types of elements deposited on the fused silica samples. This information, together with the observations of the erosion patterns of the various elements of the thruster, was enough to determine the source of the sputtering.

RESULTS

Test 1 lasted 141 hours. It was terminated because the main cathode heater developed a short. Upon removal of the thruster from the tank it was observed that the 0.025 mm thick tantalum foil heat shield for the neutralizer was eroded in one section. This erosion was caused by direct primary ion impingement which was sufficient to completely split the shield (fig. 10). Hence, the exact location of the

heat shield was not known. The view factor of the tantalum shield to the samples probably changed as the test progressed. This change could account for the variation in deposition appearance of both samples. The sputtered material pattern is shown in sketch (a).

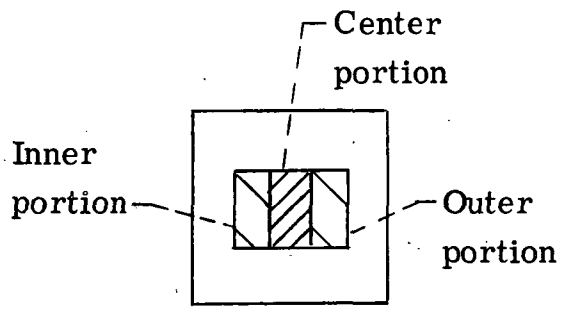

Sketch (a)

There appeared to be three sections of deposition. The film in the center portion was observed to be darker than the inner portion (closest to the neutralizer) and outer portion (furthest from the neutralizer).

The changes in spectral transmittance due to the deposition are shown in figures 11(a) to (c) for examples A and B. Figure 11(a) shows the spectral transmittance of the central portion of both samples after deposit of sputtered material as well as the spectral transmittance of the samples before exposure to sputtered material (unexposed sample). Although the numerical values of transmittance (τ) after the deposit of sputtered material at a given wavelength for samples A and B are different (for sample B, $\tau(\lambda)$ is less at all wavelengths than $\tau(\lambda)$ for sample A), the general shape of the curves are the same. This could indicate that both samples received sputtered material from the same source, but that the view factor for sputtered material of sample B probably was a little larger than for sample A. The greatest decrease in transmittance occurred in the short wavelength region between 0.40 and 0.50 μm, whereas at the long wavelengths (greater than 1.7 μm) there is less of a reduction in transmittance at a given wavelength.

The spectral transmittance of the deposition farthest from and closest to the neutralizer is given in figures 11(b) and (c), respectively. Figure 11(b) shows that the shape of the transmittance curve for the thin film deposit on the outer portions of both samples is the same. In figure 11(c), except for the data between 0.55 and 1.2 μm, the inner portions of samples A and B show the same curve shape. The total transmittance for each portion of samples A and B is tabulated in Table I. The results of the transmittance data show that the outer portions of samples A and B suffered the greatest reduction in both spectral and total transmittance. This indicates that these portions received the largest deposit of sputtered material.

Spectrographic analysis of the three coated portions indicated that each portion had nearly the same elements deposited in the same proportion. Table II lists the elements found and the relative quantity of each. Tantalum was the major element found on each part. The remaining elements, molybdenum and the components of stainless steel (chromium, iron, and nickel), were lesser constituents (minor) but still detectable. From these results, it appears that the sputtering from the neutralizer tantalum heat shield is the major thruster component detected by the samples, and hence the reduction in spectral transmittance of both samples resulted from material sputtered from the same source. It also appears that because reduction in transmittance of the outer portions of both samples A and B was significantly greater than the inner portions (see figs. 11(b) and (c)) that the tantalum heat shield tore apart and moved closer to the thruster, thus allowing the outer portions of samples A and B to receive the greatest amount of sputtered material.

By using equation (1), the resultant response of an N/P silicon solar cell located in the same plane can be calculated. The data is given in Table I, column 6, for each sputtered section of samples A and B. The reduction in solar cell output is due to the change in transmittance of the fused silicon solar cell cover plates.

The clear portion of sample A (which had a view factor that could see the glass fiber baffles and tank wall) was also spectrographically analyzed.

The only detectable elements were minute traces of aluminum, iron, titanium, and cadmium. Molybdenum, tantalum, or any of the stainless steel elements (materials found on the sputtered portions) that make up the thruster components were not detected on this portion of the sample. This result indicates that although these thruster component elements were found on the glass fiber baffles and mercury target (from other tests not included herein), they were not resputtered toward the thruster and onto the samples. This result indicates that the technique employed (glass fiber baffles, a frozen Hg target and fused silica sample in shielded holders) can detect sputtering sources with negligible background deposition, and hence the reduction in transmittance of the samples is true and due only to material sputtered from the thruster.

Test 2 was another endurance test of the translational screen-grid system. It lasted 2026 hours. Inspection of the samples revealed a thin film on sample A and an opaque film on sample B (next to the neutralizer). Sketches (b) and (c) show the patterns of samples A

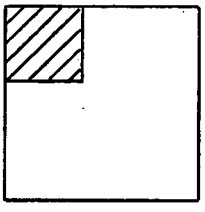

Sketch (b)
Sample A

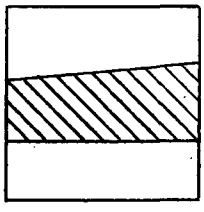

Sketch (c)
Sample B

and B, respectively, as viewed from the center of the accelerator grid. The position of the sputtered film on sample A indicated that the source of sputtering was the neutralizer. Spectrographic analysis of the sample also verified this conclusion (Table II). The optical properties of sample A are shown in figures 12(a) to (c). The spectral transmittance is given in figure 12(a). The deposition caused the greatest decrease in transmittance to occur at the shorter wavelengths. The decrease became less as the wavelength increased to about 1.25 μm. At this wavelength there was no difference (within the instrumentation

error of ±1 percent) between the data taken before and after the test. Hence, for an optical window or optical experiments on board the spacecraft, shielding from material sputtered from the neutralizer may or may not be important depending on the spectral sensitivity of the experiment. Integrating the change in spectral transmittance of sample A and normalizing to the spectral response of a N/P silicon solar cell (eq. (1)), a solar cell located in the sample plane would have a new response equal to 0.78 its original response when exposed to a thruster operating for 2000 hours.

Figures 12(b) and (c) are included to show the spectral change due to sputtering in the spectral reflectance and spectral absorptance, respectively. This type of information can be of importance to the design of thermal control of the spacecraft, because the solar absorptance of materials are determined at these wavelengths.

The integrated total optical properties between 0.398 to 2.16 μm are given in table I. Because samples A in both tests 1 and 2 had a view factor that saw sputtered neutralizer material, as indicated by spectrographic analysis, it is of interest to compare the results.

This comparison is rather difficult to make because, as was pointed out previously, the tantalum heat shield in test 1 was torn apart. This occurrence changed the view factor of the samples in test 1 and gave three distinct sputtered portions. Because the outer portion of sample A (test 1) received the greatest reduction in transmittance, this portion will be compared first. Although the length of test 1 was about 14 times shorter than the length of test 2, the reduction in total transmittance for sample A, test 1 (as shown in Table I) was $3\frac{1}{2}$ times as great as for sample A in test 2. The reduction in solar cell response was greater by a factor of three for test 1 than for test 2. The reduction in total transmittance for sample A test 1 is 50 percent greater than that of sample A test 2. The reduction in solar cell response is about 12 percent greater for A test 1 then for A test 2. The inner portion of sample A, test 1 has slightly higher values for both parameters when compared to sample A, test 2. Hence, it is apparent from both these results

that repositioning the neutralizer out of or near the beam edge (as was done in the second test so as to reduce direct impingement) will yield a smaller amount of material sputtered from the neutralizer.

The spectral transmittance of the film deposited on sample B in test 2 was measured to be zero (within the ±1 percent accuracy of the instrumentation) for all wavelengths, indicating that a total opaque film was deposited on the surface. Any optical element or solar cell would be rendered inoperative due to this deposit. The spectral reflectance and absorptance are shown in figures 13(a) and (b), respectively. The reference properties (before exposure to sputtered material) are also given in both figures. The spectral reflectance of the film on sample B has an entirely different trend than the spectral reflectance found on sample A (test 2) and the unexposed sample. The spectral reflectance of sample B increases almost linearly from 0.2 to 0.45 as the wavelength increases from 0.4 to 2.16 μm. The reference data (initial reflectance) has almost constant value (about 0.05) for all wavelengths, while the data of sample A of test 2 showed a decrease in spectral reflectance with increasing wavelength (ρ = 0.62 at 0.4 μm and ρ = 0.08 at 2.16 μm). The spectral absorptance (fig. 13(b)), which is $1 - \rho(\lambda)$ (since $\tau = 0$ at all wavelengths) decreases as the wavelength increases. These trends in spectral reflectance and absorptance for the wavelengths considered are usually indicative of a totally opaque film or for semi-infinite materials (ref. 4) rather than of thin films. Visual observation and the transmittance measurement indicate that the deposition is opaque (greater than 400 Å thick). The values of absolute transmittance, reflectance, and absorptance before and after the test are given in Table I. Also listed is the change of each property due to the film deposition.

Spectrographic analysis revealed the elements given in Table II. Molybdenum was the major component. The elements of stainless steel (iron and nickel) were also present. The presence of mercury was unexpected and as yet unexplained. Examination of the accelerator grid showed the erosion pattern depicted in figure 14. The sputtering is caused by charge exchange mercury ions falling on the accelerator electrode (ref. 5). This type of sputtering cannot be eliminated entirely

(ref. 6). Although thruster operation in the 10^{o} vectored mode is not contemplated presently for flight operation, the results show that the sputtering while in this mode could be damaging and precautions against this damage should be taken.

It should be pointed out that these data apply to the translational screen-grid system. Other extraction configurations may have different characteristics.

CONCLUDING REMARKS

Results of the present study indicate that fused silica samples, properly shielded from backsputtered material from vacuum tank walls, can be useful in detecting the source of materials sputtered from an ion thruster. By means of a spectrographic analysis, after termination of a test, it is possible to analyze the type of material sputtered on the fused silica samples. Knowing the view factor of each sample along with the knowledge of various components of the ion thruster allows the determination of the source of sputtered material.

These measurements, along with transmittance measurements of the samples both before and after exposure to the sputtered material, allows one to determine the necessity of reducing the effects of the sputtered material on optical windows and solar cells aboard the spacecraft.

It was found in the present experiments that proper location of the neutralizer with respect to the beam edge is important. With the neutralizer immersed in the beam as in the first test, the sputtered tantalum deposited on a fused silica solar cell cover could reduce the response of a N/P silicon solar cell by as much as a factor of thirteen in the same period of time when compared to the neutralizer located near the edge of the beam in the second test. Comparison of total transmittance measurements for the neutralizer locations in tests 1 and 2 indicate a factor of as much as fourteen in reduction of total transmittance.

The results of the 2026-hour test also indicated that with translation vectored grids, material sputtered from the accelerator grid was of sufficient magnitude to render totally opaque between 0.398 and 2.16 μm a fused silica sample located in the opposite direction of the vectored beam. Thus, depending on the time the thruster is in the vectored mode, proper baffling may be necessary as a shield from the sputtered material.

REFERENCES

1. Lathem, Walter C.: Grid-Translation Beam Deflection Systems for 5-cm and 30-cm Diameter Kaufman Thrusters. Paper 72-485, AIAA, Apr. 1972.

2. Bowman, R. L.; Mirtich, M. J.; and Weigand, A. J.: Changes in Optical Properties of Various Transmitting Materials Due to Simulated Micrometeoroid Exposure. Presented at the Optical Society of America Annual Meeting, Chicago, Ill., Oct. 21-24, 1969.

3. Cooley, William C.; and Barrett, Matthew J.: Handbook of Space Environmental Effects on Solar Cell Power Systems. Exotech, Inc. (NASA CR-100327), Jan. 1968.

4. Spisz, Ernie W.; Weigand, Albert J.; Bowman, Robert L.; and Jack, John R.: Solar Absorptances and Spectral Reflectances of 12 Metals Ranging from 300 to 500 K. NASA TN D-5353, 1969.

5. Lathem, Walter C.: Analytic Performance of Two-Grid Accelerator Designs for Kaufman Thrusters. NASA TN D-6275, 1971.

6. Kaufman, Harold R.; Cohen, Allen J.: Maximum Propellant Utilization in an Electron-Bombardment Thruster. Presented at the Symposium on Ion Sources and Formation of Ion Beams, Brookhaven National Laboratory, Upton, N. Y., Oct. 19-21, 1971.

TABLE I. - TABULATED DATA AND RESULTS

Test, hr	Sample	Total optical property	Percent degradation of total transmittance due to deposition, $\frac{\tau_{ref} - \tau_{sample}}{\tau_{ref}}$	Response of 10 ohm-cm N/P silicon solar cell	Resultant output of 10 ohm-cm N/P silicon solar cell, $\frac{sample}{ref}$
141	A Center	$\tau = 0.633$	0.317	0.647	0.691
	Inner	.738	.204	.747	.799
	Outer	.244	.737	.227	.242
141	B Center	$\tau = 0.549$	.408	.558	.596
	Inner	.641	.308	.629	.672
	Outer	.323	.652	.302	.324
2026	A	$\tau = 0.731$ $\rho = .236$ $\alpha = .033$	.211	.730	.780
2026	B	$\tau = 0.00$ $\rho = .711$ $\alpha = .289$			
	Reference (Unexposed sample)	$\tau = 0.927$		.936	

O Release

TABLE II. - ELEMENTS SPECTROGRAPHICALLY DETECTED ON FUSED SILICA SAMPLES

Test, hr	Sample	Element detected	Relative quantity
141	A (All sections)	Tantalum	Major
		Molybdenum	Minor
		Iron	Minor
		Chromium	Minor
		Nickel	Trace
141	B (All sections)	Tantalum	Major
		Molybdenum	Minor
		Iron	Minor
		Chromium	Minor
		Nickel	Trace
2026	A	Tantalum	Major
		Molybdenum	Trace
2026	B	Molybdenum	Major
		Nickel	Minor
		Iron	Minor
		Mercury	Minor
		Tantalum	Trace

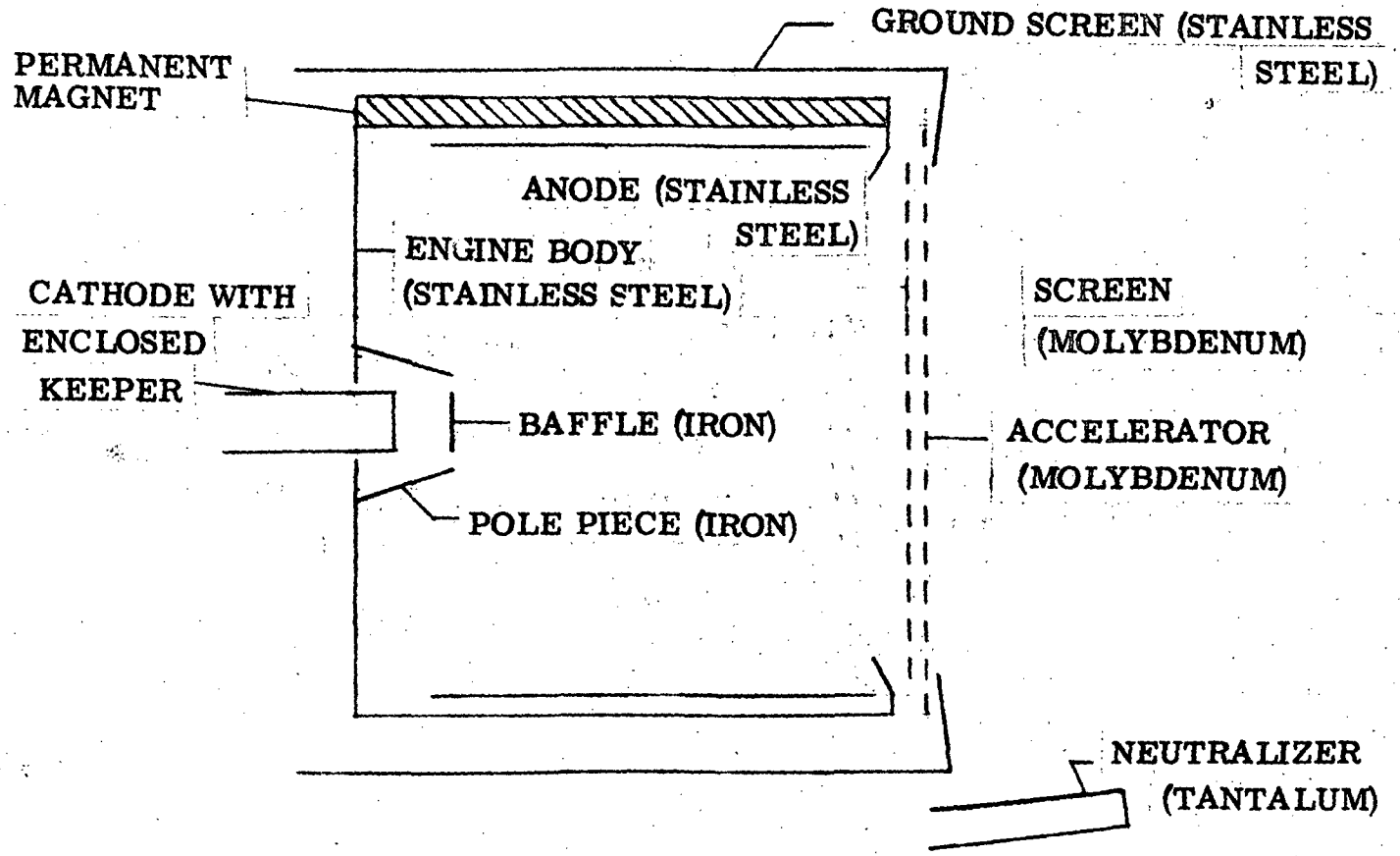

Figure 1. - Components of 5-cm diameter ion thruster.

THERMOMECHANICAL 5-CM VECTORABLE GRID

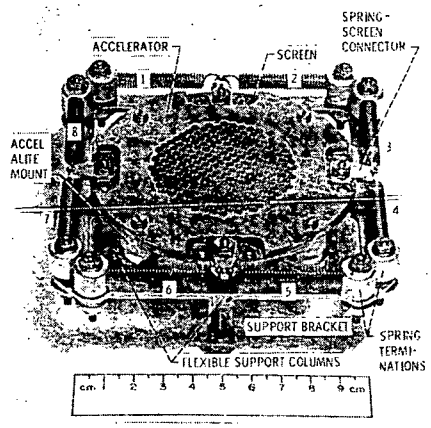

CS-62614

Figure 2. - Translational screen-grid vectoring system.

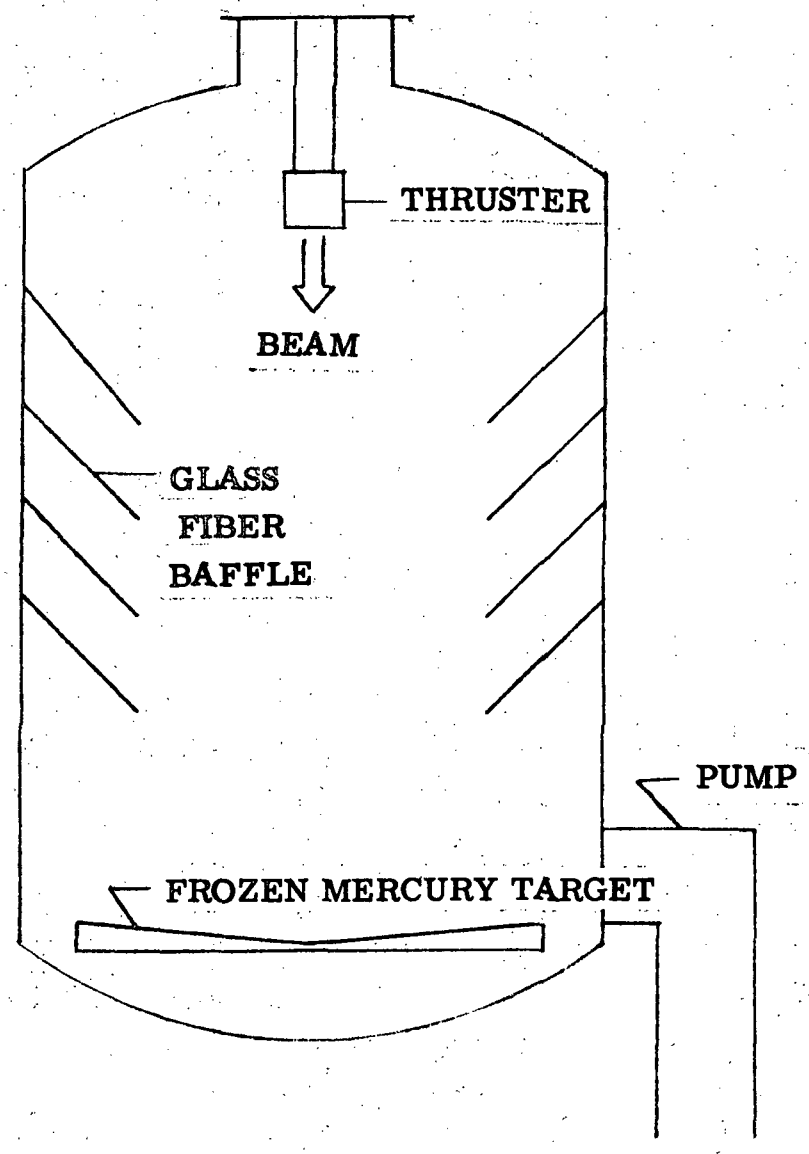

Figure 3. - Vacuum tank.

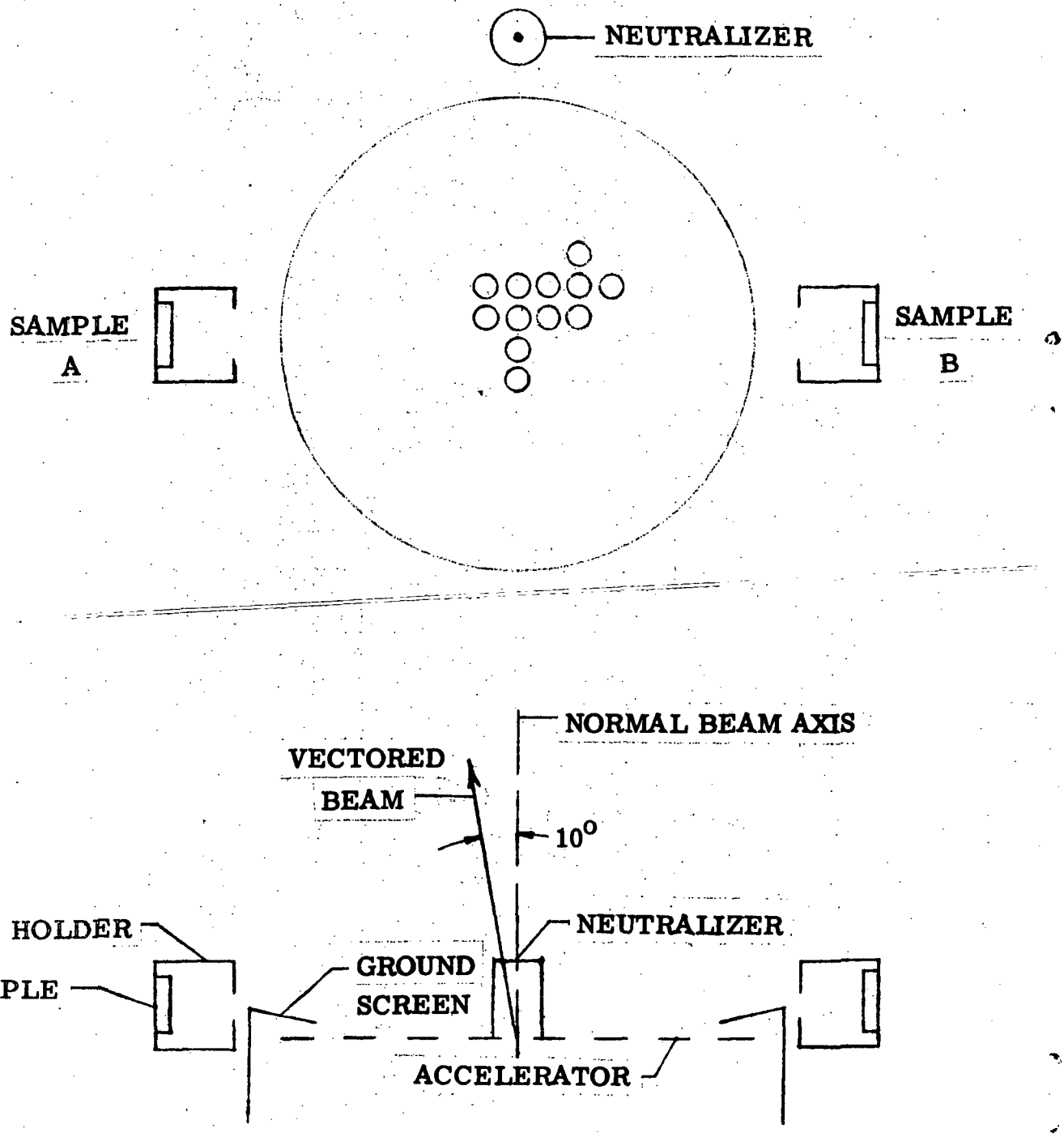

Figure 4. - Sample locations for Test 1.

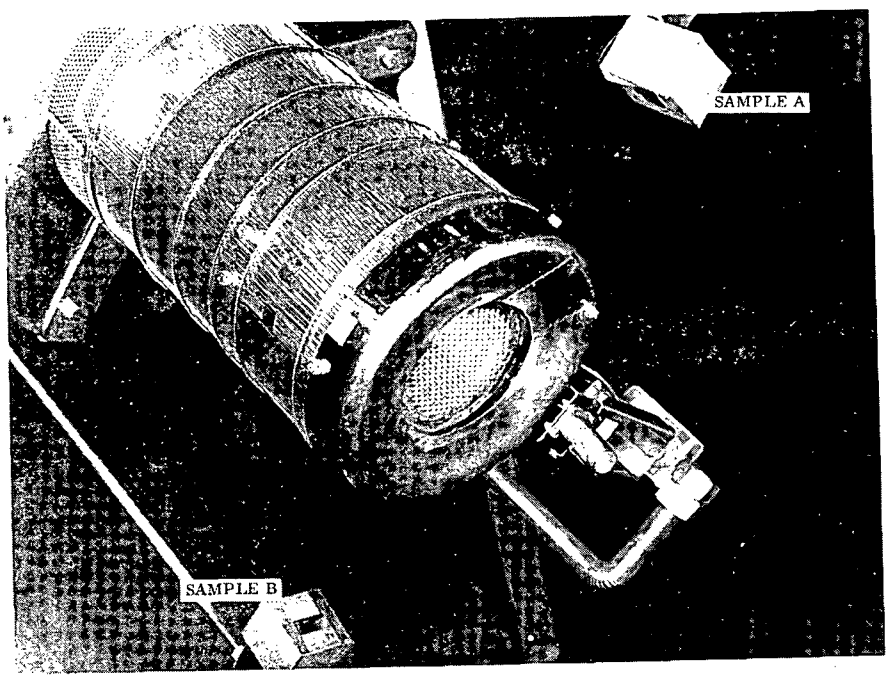

Figure 5. - Photograph of sample locations for Test 1.

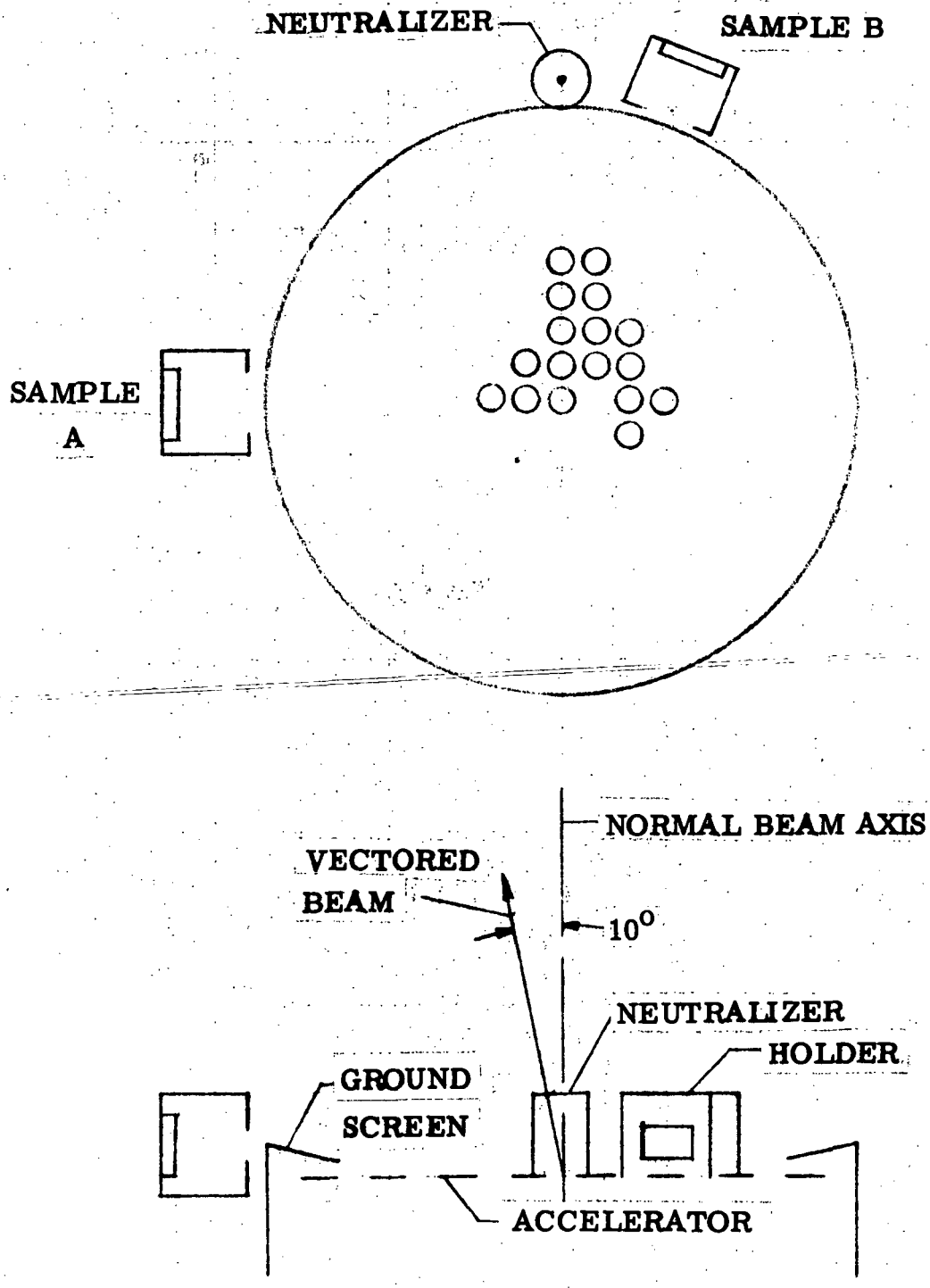

Figure 6. - Sample locations for Test 2.

E-6764

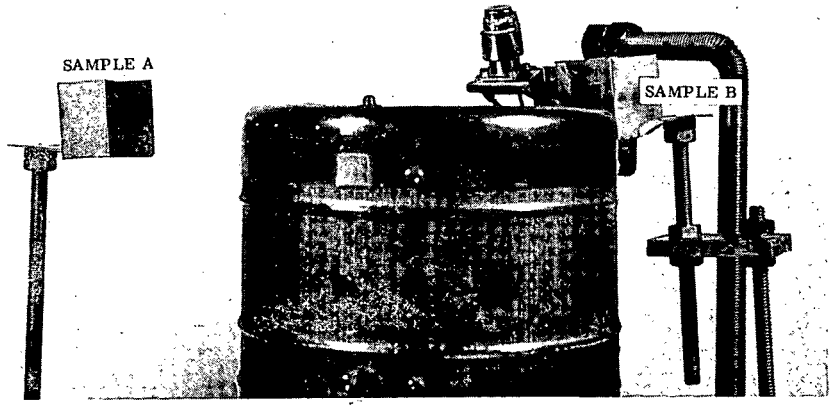

Figure 8. - Photograph of sample locations for Test 2 (along ground screen plane).

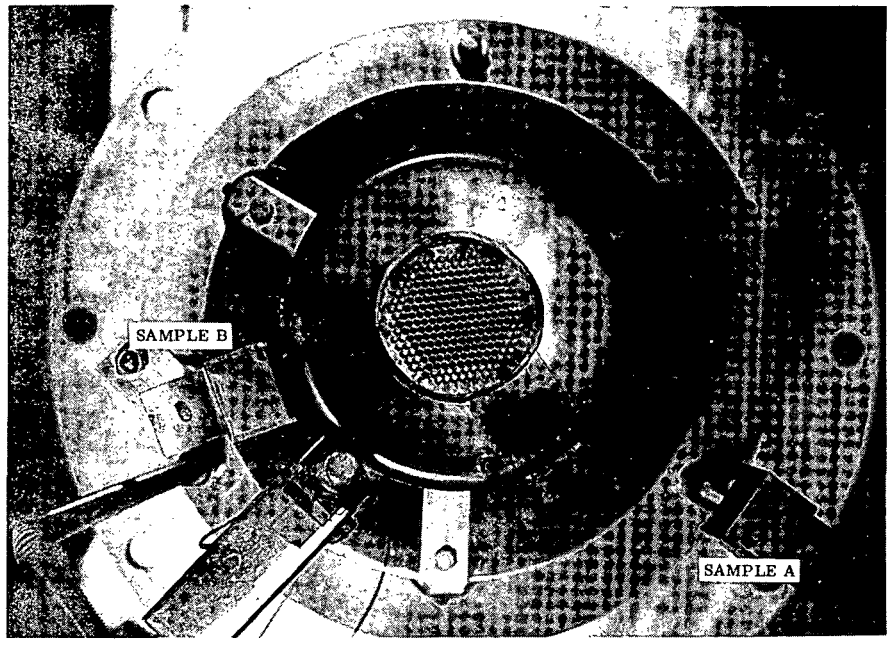

Figure 7. - Photograph of sample locations for Test 2 (looking upstream along the thruster axis).

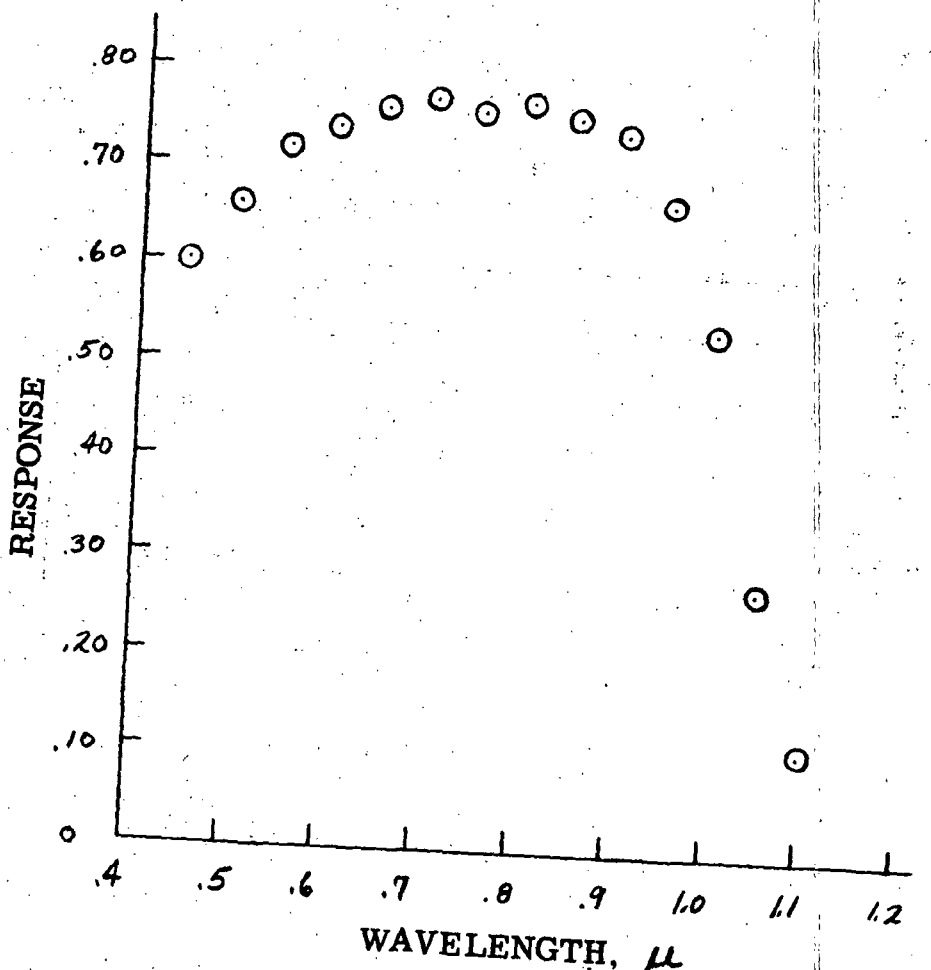

Figure 9. - Spectral response of a 10-ohm-cm N/P silicon solar cell.

E-6964

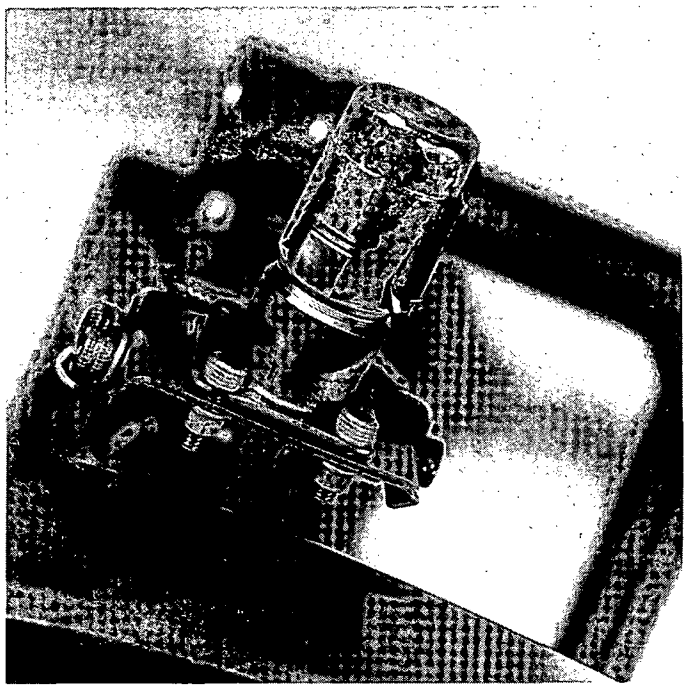

Figure 10. - Neutralizer after Test 1.

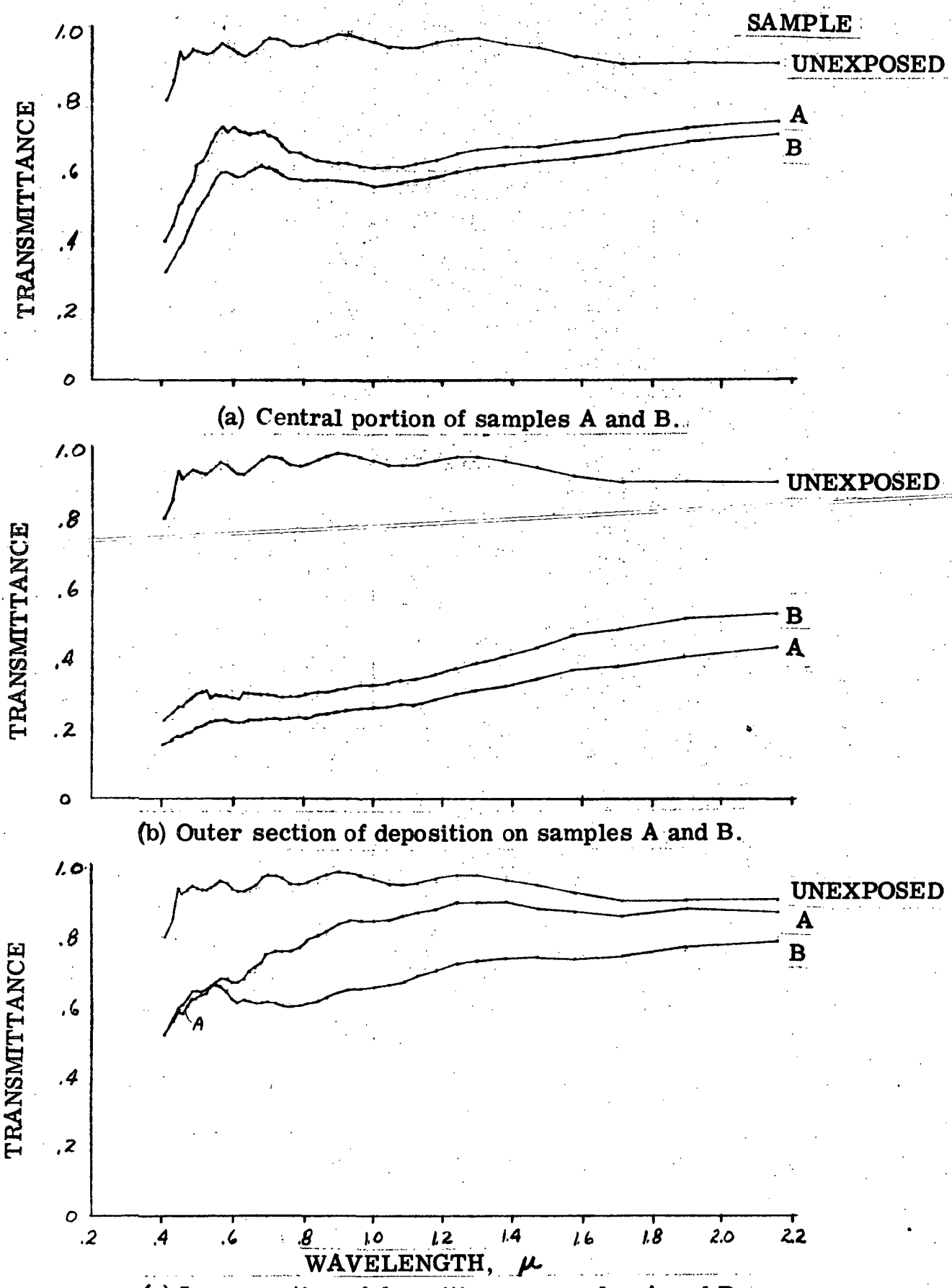

Figure 11. - Spectral transmittance of various locations on samples A and B of Test 1.

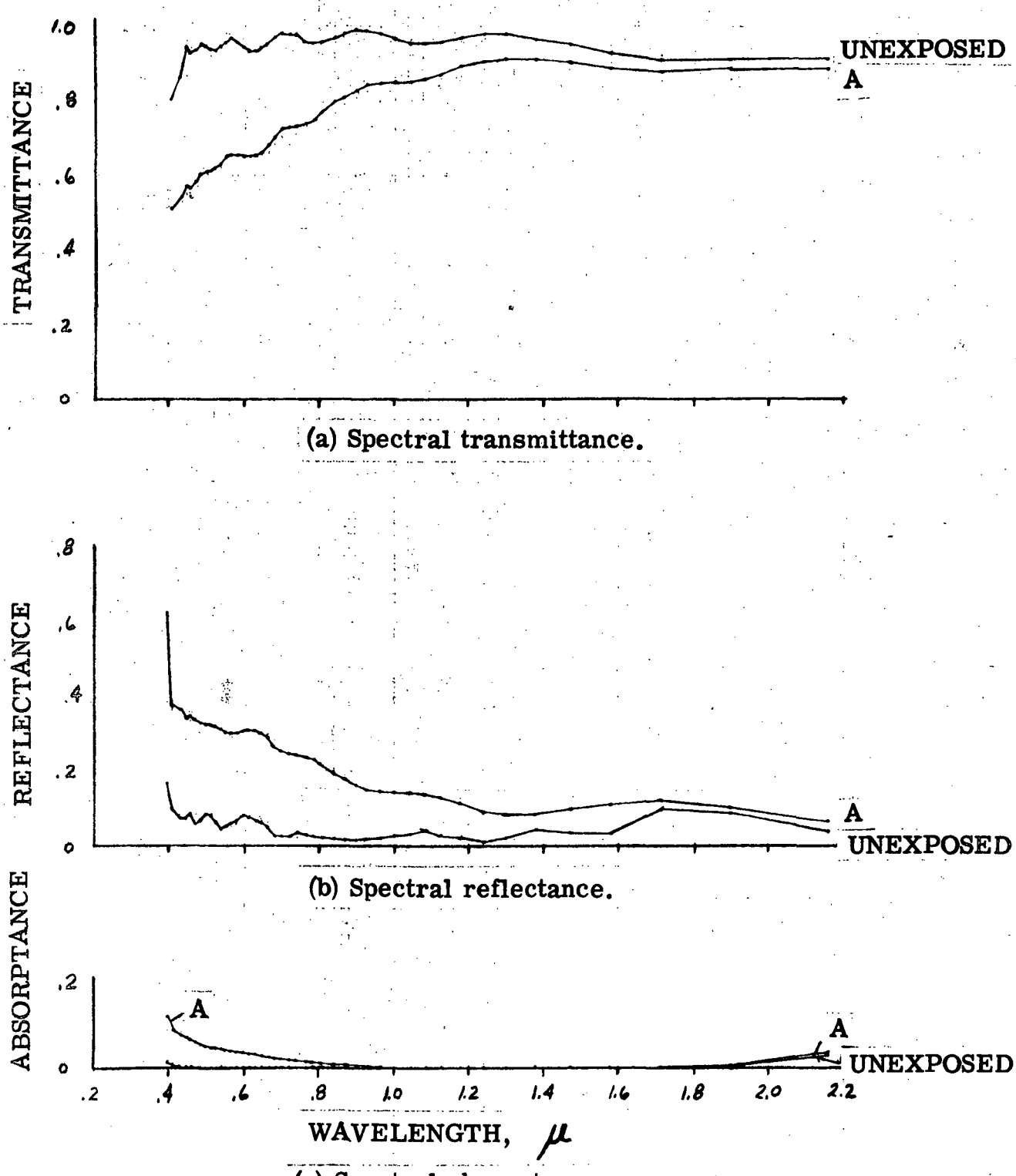

(a) Spectral transmittance.

(b) Spectral reflectance.

(c) Spectral absorptance.

Figure 12. - Optical properties of sample A deposition from Test 2.

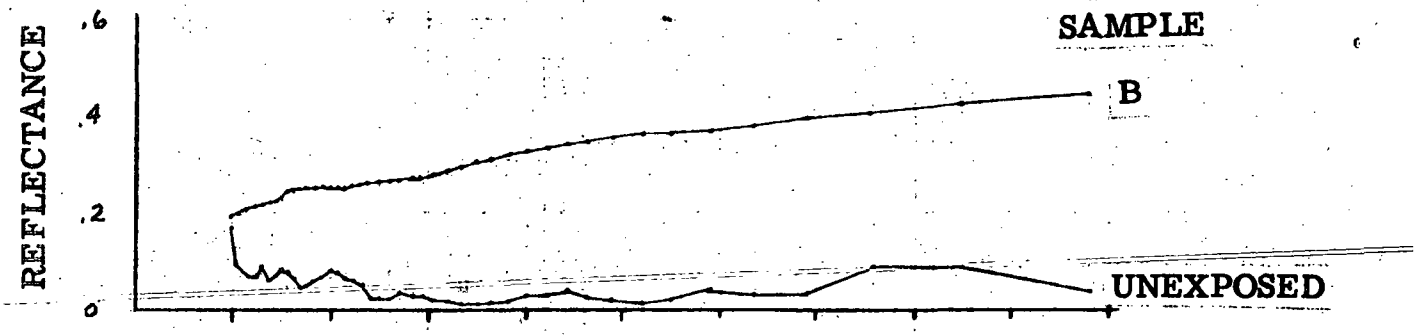

(a) Spectral reflectance.

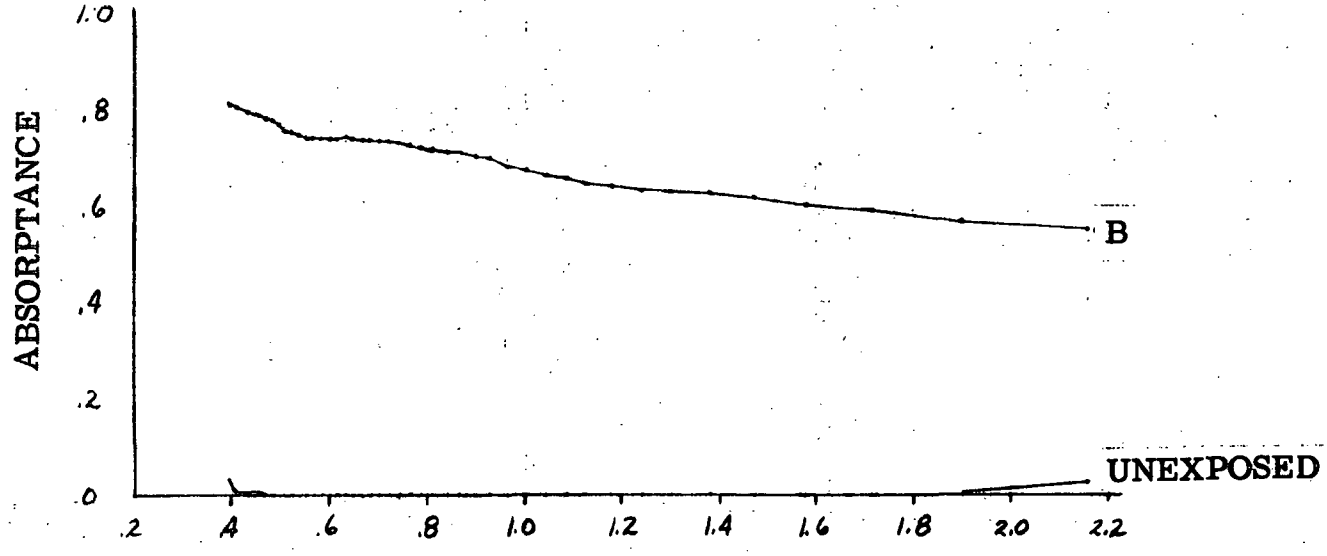

(b) Spectral absorptance.

Figure 13. - Optical properties of sample B from Test 2 (τ = 0 at all wavelengths).

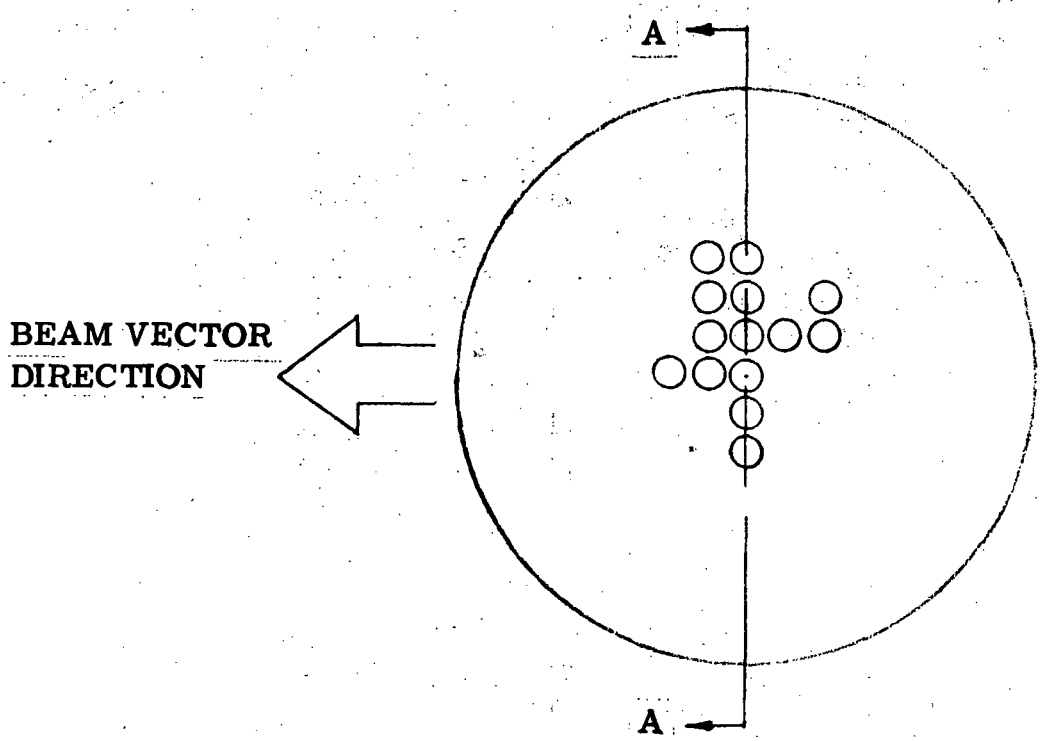

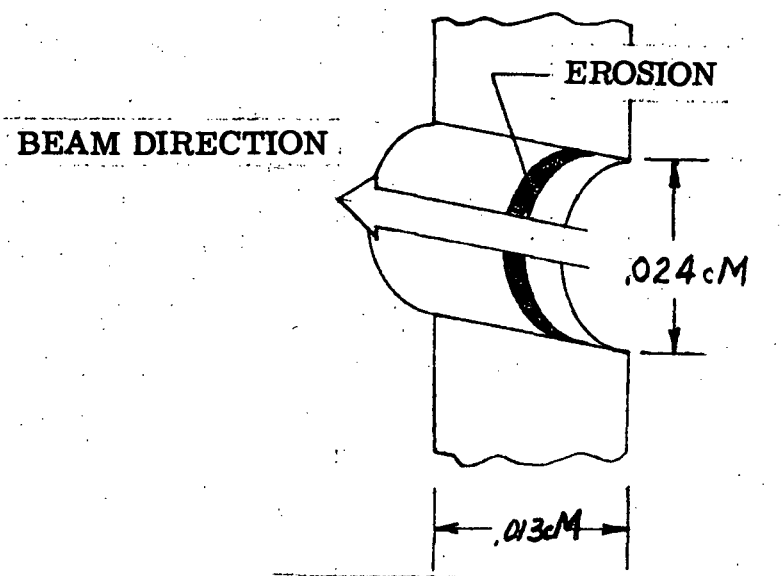

Isometric view of section A-A

Figure 14. - Accelerator grid erosion of Test 2.